HHS Public Access

Author manuscript

J Proteome Res. Author manuscript; available in PMC 2018 August 04.

Published in final edited form as:

J Proteome Res. 2017 August 04; 16(8): 2729–2742. doi:10.1021/acs.jproteome.6b01026.

A PLC-γ1 Feedback Pathway Regulates Lck Substrate Phosphorylation at the T Cell Receptor and SLP-76 Complex

Judson Belmont[†,‖], **Tao Gu**[†,‖], **Ashley Mudd**[†], and **Arthur R. Salomon**[†,‡,*]

[†]Department of Molecular Biology, Cell Biology, and Biochemistry, Brown University, Providence, RI 02912, USA

[‡]Department of Chemistry, Brown University, Providence, RI 02912, USA

Abstract

Phospholipase C gamma 1 (PLC-γ1) occupies a critically important position in the T cell signaling pathway. While its functions as a regulator of both Ca^{2+} signaling and PKC-family kinases are well characterized, PLC-γ1's role in the regulation of early T cell receptor signaling events is incompletely understood. Activation of the T cell receptor leads to the formation of a signalosome complex between SLP-76, LAT, PLC-γ1, Itk, and Vav1. Recent studies have revealed the existence of both positive and negative feedback pathways from SLP-76 to the apical kinase in the pathway, Lck. To determine if PLC-γ1 contributes to the regulation of these feedback networks, we performed a quantitative phosphoproteomic analysis of PLC-γ1-deficient T cells. These data revealed a previously unappreciated role for PLC-γ1 in the positive regulation of Zap-7 and T cell receptor tyrosine phosphorylation. Conversely, PLC-γ1 negatively regulated the phosphorylation of SLP-76-associated proteins, including previously established Lck substrate phosphorylation sites within this complex. While the positive and negative regulatory phosphorylation sites on Lck were largely unchanged, Tyr^{192} phosphorylation was elevated in Jgamma1. The data supports a model wherein Lck's targeting, but not its kinase activity, is altered by PLC-γ1, possibly through Lck Tyr^{192} phosphorylation and increased association of the kinase with protein scaffolds SLP-76 and TSAd.

Keywords

Phosphoproteomics; LC/MS; label-free quantitation; T cell signaling; PLC-γ1; SLP-76; Lck

Introduction

In response to antigenic stimulation, CD4+ T cells undergo transcriptional, biochemical, and morphological changes to enable them to carry out their immune defense functions. At the intracellular level, these functions are regulated by tightly coordinated signaling cascades. The generation of an immune response of proper strength and duration requires careful coordination of signal transduction machinery, since autoimmune or immunodeficiency disorders can occur when competing biochemical signals are improperly balanced.

*for correspondence: Tel: (401) 863-6091, as@brown.edu.

‖These authors contributed equally

Although many of the details of early T cell signaling remain to be elucidated, it is now understood that a dynamic tyrosine phosphoproteome underlies many of the significant events in early T cell activation. Initiation of T cell signaling occurs when a cognate peptide-major histocompatibility complex engages with the T cell receptor (TCR), resulting in clustering of the cytoplasmic tails of the receptor subunits as well as recruitment of the Src family kinase Lck. Once recruited there, Lck phosphorylates immunoreceptor tyrosine-based activation motifs (ITAMs) located on the ζ and CD3 subunits of the receptor.[1] The phosphorylated CD3 and ζ ITAMs provide a docking site for the SH2 domains of the Syk family kinase Zap-7, which becomes activated through both autophosphorylation and modification by Lck.[2–4] Subsequently, Zap-7 and Lck kinase activity promote the activation of downstream signaling modules through their interactions with a multiprotein signalosome complex nucleated by SH2 domain-containing leukocyte phosphoprotein of 76 kDa (SLP-76) and LAT.[5] Assembly and phosphorylation of proteins within the signalosome contributes critically to a variety of downstream effects, including mobilization of Ca^{2+}, cytoskeletal reorganization, activation of MAPK pathways, modulation of protein kinase C (PKC) signaling, and activation of transcriptional programs.[5–9]

Phospholipase C-γ1 (PLC-γ1) is a member of the Phospholipase C family of enzymes that is widely expressed throughout many tissues.[10] During T cell activation, Itk phosphorylates PLC-γ1 on Tyr^{783} to reorient the active site into an open conformation.[10–12] In this conformation, PLC-γ1 catalyzes the cleavage of phosphatidylinositol 4,5-bisphosphate (PIP_2) to inositol 1,4,5-trisphosphate (IP_3) and diacylglycerol (DAG).[10] Both DAG and IP_3 function as essential second messengers in the transduction of T cell signaling: DAG is a cofactor for various PKC-family enzymes, while IP_3 regulates release of Ca^{2+} from the ER.[10] PLC-γ1 and its related isoform, PLC-γ2, are distinguished from the rest of the phospholipase C family by the presence of tandem SH2 domains, which are essential for PLC-γ1's functionality and activation, as well as an SH3 domain, which mediates the constitutive interaction of PLC-γ1 with the proline-rich region of SLP-76 in resting T cells.[13–15] Both PLC-γ1 and PLC-γ2 contain an N-terminal PH domain that is characteristic of most phospholipase C enzymes and allows for recruitment of the enzymes to PIP_3 in the membrane.[16] Like PLC-γ1, PLC-γ2 is also positively regulated by Itk phosphorylation of Tyr^{759} that allows for an intramolecular interaction between the phosphorylated residue and the C-terminal SH2 domain.[17–18] Despite its structural similarities to PLC-γ1, however, PLC-γ2 is more narrowly expressed, being restricted primarily to hematopoietic lineages, and has previously been shown to incompletely compensate for loss of PLC-γ1.[1, 19]

Phospholipase C signaling has far-reaching consequences in cell spreading and metastasis as well as thymocyte development and T-cell activation. PLC-γ1 has been shown to promote chemotaxis via modulation of Rac and CDC42 activity, and elevated expression of PLC-γ1 is a commonly observed signature of metastatic tumors.[20–22]. In mice, conditional deletion of PLC-γ1 in thymocytes produces a profound block in both positive and negative selection during development.[23] These mice also experience an increased prevalence of autoimmune disorders as well as a substantial reduction in peripheral T cells, reportedly due to an elevated rate of activation-induced cell death.[23] Additionally, T cells that do successfully mature in these lines exhibit defects in proliferation and cytokine production in response to antigen stimulation.[14, 23] At the intracellular level, PLC-γ1 is required in mature T cells for

sustained increases in intracellular Ca^{2+} as well as activation of Erk, Jnk, and the transcription factors NFAT, AP-1, and NF-κB.[14, 23] The defect in Ca^{2+} signaling observed in PLC-γ1 cells is not absolute, as these cells still exhibit a transient increase in Ca^{2+} in response to TCR engagement.[14] This has led to speculation that PLC-γ2 expressed in T cells may be sufficient for temporary, but not sustainable, elevation of intracellular Ca^{2+};[19] however, it is presently unknown whether the incompleteness of this compensation is due strictly to the comparatively lower levels of PLC-γ2 expressed in T cells or whether PLC-γ1 and PLC-γ2 carry out non-redundant functions in T cell signaling.[24–25]

While the significance of PLC-γ1 in TCR signal transduction is widely recognized, its role in regulating the receptor-proximal phosphorylation events that govern the pathway is not well understood. Recent studies have revealed the existence of both positive and negative feedback pathways from components of the signalosome complex to the apical kinase in the pathway, Lck. N terminal tyrosine residues of SLP-76 regulate a negative feedback pathway early and positive feedback pathway late after receptor stimulation to the activation site on Lck, Tyr^{394}, and the substrates of active Lck, including the CD3 and ζ ITAMs and ZAP-7.[26–27] Another study showed that Vav1 regulates a negative feedback pathway to Lck Tyr^{394} as well as the CD3 and ζ ITAMs and ZAP-7.[28] In the present study, we performed an LC-MS/MS-based quantitative phosphoproteomic analysis to identify altered phosphorylation during early T cell signaling in a PLC-γ1-deficient cell line, Jgamma1, and its PLC-γ1-reconstituted counterpart. Our data reveal a widespread dependence on PLC-γ1 for hundreds of sites across the tyrosine phosphoproteome. Notably, these sites include known regulatory residues on Lck, Zap-7, and Itk, as well as many more sites on established targets of Lck. These observations both reaffirm the centrality of PLC-γ1 to T cell functionality and suggest that events in the signaling pathway as early as the TCR stimulation-induced phosphorylation of ITAM sites are regulated by PLC-γ1. Furthermore, our data point to a previously uncharacterized mechanism through which PLC-γ1 regulates the activity and targeting of Lck.

Materials and Methods

Cell culture and T cell stimulation

The PLC-γ1 deficient cell line Jgamma1 (ATCC#CRL-2678) and its reconstituted counterpart Jgamma1.WT (ATCC# CRL-2679)[14] were obtained from American Tissue Culture Collection (ATCC, Manassas, VA). Both cell lines were cultured in RPMI 1640 medium (Hyclone, Logan, UT) supplemented with 10% heat-inactivated FBS (Hyclone, Logan, UT), 2mM L-glutamine, 100U/ml penicillin G, and 100μg/ml streptomycin (Invitrogen, Carlsbad, CA) in a humidified incubator with 5% CO_2 at 37°C.

The TCR stimulation was performed as previously described[29] by treating with anti-CD3 and anti-CD4 (clones OKT3 and OKT4; eBioscience, San Diego, CA). For each replicate and time point, 1×10^8 cells were treated with 2.5μg/ml each of anti-CD3 and anti-CD4 antibodies for 30 seconds at 37°C. Cells were then treated with 22μg/ml of goat anti-mouse IgG (Jackson ImmunoResearch, West Grove, PA) to cross-link OKT3/4 before incubation at 37°C for 0, 1, 2, 3, 5, or 10 minutes. Stimulation was halted with the addition of lysis buffer (8M urea, 20mM HEPES, 2.5mM sodium pyrophosphate, 1mM sodium orthovanadate,

1mM β-glycerophosphate, pH=8.0) followed by a 30 minute incubation at 4°C. Lysates were sonicated at a 30watt output with 3 bursts of 30 seconds each and cleared by centrifugation at 12,000×g for 15 minutes at 4 °C.

Protein reduction, alkylation, digestion and peptide immunoprecipitation

Protein reduction and alkylation were performed as previously described.[30] Trypsin digestion was also performed according to a previously detailed protocol[30], but with TPCK-treated trypsin (Worthington, Lakewood, NJ) substituted and used in a 1:1 (w/w) trypsin:protein ratio. Tryptic peptides were acidified, cleared, and desalted using C18 Sep-Pak plus cartridges (Waters, Milford, MA) in accordance with a previously described protocol,[30] then lyophilized for 48 hours.

Prior to peptide immunoprecipitation, a 10 pmol fraction of a synthetic phosphopeptide (LIEDAEpYTAK) was spiked in to each sample to serve as a quantitation standard. Peptide immunoprecipitation was performed using a previously detailed protocol[30] employing p-Tyr-1 phosphotyrosine antibody beads (Cell Signaling Technology). After washing, peptides were eluted from the beads with 0.15% TFA and desalted via C18 Zip Tip pipette tips (Millipore Corporation Billerica, MA) as previously described.[31] Five biological replicates of each time point were prepared for the phosphoproteomic investigation of each cell line.

Automated nano12LC/MS

Phosphopeptides were loaded from an Agilent 1200 G1367B high performance Autosampler to a C18 precolumn in accordance with a previously detailed method,[30] with the exception that the precolumn and analytical column in the current study were packed with 2cm of 3-μm C18 particles, and an electrospray voltage of 2.0kV was applied to the flow path via platinum wire using an Upchurch MicroTee (IDEX Health & Science, Oak Harbor, WA) between the precolumn and analytical column.

MS spectra were acquired on a Q Exactive mass spectrometer (Thermo Fisher Scientific, Waltham, MA) using parameters detailed previously,[34] with the exception that the ion selection abundance threshold was set at 1.0×10^3.

Data analysis

Data analysis was performed using a custom phosphoproteomic software platform.[35–36] MS/MS spectra were searched against a custom database comprised of the 87,613 forward protein sequences contained in the non-redundant human UniProt complete proteome set database (2/1/2013) and an equal number of reversed decoy entries using the Mascot algorithm (version 2.4.0, Matrix Science).[37] Peak lists were generated using Proteowizard's msconvert software (version 3.0.4888) and default parameters with the MS2Deisotope filter. The following parameters were used for the Mascot database search: trypsin enzyme cleavage specificity, 2 possible missed cleavages, 10 ppm mass tolerance for precursor ions, 50 mmu mass tolerance for fragment ions. Search parameters specified a variable modification of phosphorylation (+79.9663 Da) on serine, threonine, and tyrosine residues, a variable modification of methionine oxidation (+15.9949 Da), and a static modification of carbamidomethylation (+57.0215 Da) on cysteine. To validate sequence assignment of

phosphopeptides, a logistic spectral score[35] filter was applied to attain a final estimated decoy database false discovery rate (FDR) of 1%. FDR was estimated via the decoy database approach following the collation of non-redundant data into heatmaps.[38] To ensure high confidence in the assigned positions of phosphorylation sites, the Ascore algorithm[39] was applied to each phosphopeptide spectrum match, and the top Ascore prediction was used as the reported phosphorylation site position.

Quantitation of Relative Phosphopeptide Abundance

Label-free quantitation of relative phosphopeptide abundance was achieved by integrating selected ion chromatogram (SIC) peak areas for all phosphopeptides. Retention time alignment of individual replicate analyses was performed as described previously, as was calculation of peak areas using a previously established in-house software package updated for compatibility with Xcalibur Development Kit 2.2 SP1 (Thermo Fisher Scientific).[40] The peak area of the spiked-in LIEDAEpYTAK phosphopeptide was used as a normalization factor for each individual SIC peak area during quantitation.

Two different heatmaps were generated for each peptide observed in the data: an abundance heatmap showing the amount of phosphopeptide detected in a cell line, and a ratio heatmap indicating the fold change in phosphopeptide abundance between the two cell lines. Abundance heatmaps were generated for the Jgamma1.WT across the timecourse of TCR stimulation.[41] Each individual heatmap square color was generated from the average of the standard phosphopeptide-normalized SICs from five biological replicate experiments. In the abundance heatmap representation, the geometric mean of a given phosphopeptide abundance across all time points was set to the color black. A blue color represented below average abundance, while yellow represented above average abundance for each unique phosphopeptide across the timecourse. Blank squares in the heatmap indicated that no clearly defined SIC peaks were observed for that phosphopeptide in any of the replicate analyses at that time point. p values were calculated from the replicate data using a two-sample t-test comparing each time point to the time point with the minimum average peak area for that phosphopeptide. To adjust for multiple hypothesis testing, q values were subsequently calculated for each time point using the R package QVALUE as previously described.[42–43] A white dot on an abundance heatmap square indicated that a significant difference ($q < 0.05$) was detected for that phosphopeptide and timepoint relative to the timepoint with the minimal value.

In the ratio heatmap, the ratios of phosphopeptide abundances between the Jgamma1 and Jgamma1.WT cell lines for each timepoint within the time course of TCR stimulation were represented. For the ratio heatmap, a black color represented a ratio of 1 between the Jgamma1 and Jgamma1.WT cells at that time point. A red color represented lower abundance, while a green color represented higher abundance of the given phosphopeptide in Jgamma1 cells compared with the Jgamma1.WT cells. The magnitude of change of the heatmap color was calculated as described.[41] Two-sample t-tests were performed to identify changes in abundance between the Jgamma1 and Jgamma1.WT cells for each phosphopeptide and time point, and q values were subsequently calculated to control the FDR. A white dot on a heatmap square indicated that a significant change ($q < 0.05$) was

observed between the replicate data from the Jgamma1 and Jgamma1.WT cells samples for that time point and phosphopeptide.

Hierarchical clustering

Hierarchical clustering was performed using Cluster 3.0[44] and visualized with TreeView 3.0.[45] Input to the hierarchical clustering algorithm is a 195×6 matrix of phosphopeptide peak areas, where 195 is the number of peptides from our phosphoproteomic dataset selected for clustering, and each row consists of the log2-transformed ratios of average peptide peak areas between Jgamma1 and Jgamma1.WT at the 6 timepoints sampled. To be selected for clustering, a peptide had to be derived from a protein containing either one or more Lck-phosphorylated sites documented in the PhosphoSitePlus database,[46] or one or more sites within an Lck kinase motif predicted at high stringency in Scansite.[47] Peptides derived from Lck are included in the analysis due to the prevalence of Lck autophosphorylation during TCR signaling. Additional peptides were included based on in-house manual curation of known Lck substrates. For hierarchical clustering, Pearson correlation coefficient was used as the distance metric, and clusters distances were assessed based on average linkage.

Western blotting

Cell lysates prepared with 8 M urea were diluted 1:1 with sample loading buffer (20% v/v glycerol, 5% 2-mercaptoethanol, 4% SDS, 125 mM Tris-HCl, pH 6.8, 0.01% bromophenol blue) for each proteomic sample. Following a DC protein assay, equal amounts of protein were separated by 4–2 % gradient SDS-PAGE on Precise Tris-HEPES gel (Thermo Fisher Scientific), and electroblotted onto Immobilon membranes (Millipore, Billerica, MA). Membranes were blocked in Odyssey blocking buffer for 30 minutes at RT (Li-Cor, Lincoln, NE) and then incubated with primary antibody overnight at 4°C. Membranes were washed 3 times for 5 minutes at RT in PBS/0.1% Tween-2, incubated with IgGs conjugated with an IRDye (Li-Cor) for 45 minutes, then washed again. Bands were visualized using an Odssey Imaging System (Li- Cor). Antibodies to CD3ε, PLC-γ1, Zap-7, and phospho-Zap-7 (Tyr319 and Ty493) were obtained from Cell Signaling Technologies. Antibody to TCRζ was obtained from Santa Cruz Biotechnology. Antibody to GADPH was obtained from Sigma-Aldrich. Antibody to Itk was obtained from Thermo Fisher.

Results

A quantitative, bottom-up phosphoproteomic strategy was used to compare the phosphotyrosine profiles of Jurkat PLC-γ1-deficient cells (Jgamma1) and PLC-γ1-reconstituted cells (Jgamma1.WT). After validating the PLC-γ1 deficiency and reconstitution of the Jgamma1 and Jgamma1.WT cell lines respectively (Figure S1), samples were taken from each cell line at six timepoints ranging from 0–1 minutes following stimulation of the cells with OKT3 crosslink. For each time point and cell line, five biological replicates were analyzed by LC-MS/MS. The resulting phosphoproteomic data represents an unbiased, wide-scale view of the dynamic tyrosine phosphoproteome during early TCR signaling in the presence and absence of PLC-γ1.

After processing the phosphoproteomic samples and obtaining raw MS/MS spectra, high confidence sequence assignments were made as described in the Materials and Methods section. Relative abundance of each phosphopeptide at each time point was calculated by integrating SIC peak areas. A complete list of identified phosphopeptides and their associated SIC peak areas and statistics (Table S1) and all LC/MS-specific peptide data including MOWSE score and Ascore (Table S2) are available. The raw LC/MS data (Thermo Fisher raw format) and assigned MSMS spectra (pepXML) for all peptides have been submitted to the ProteomeXchange (http://proteomecentral.proteomexchange.org) via the PRIDE partner repository with the dataset identifier PXD005165.[48–49] Annotated MSMS spectra for all PTM-containing peptides from this study are provided as supporting information (Figure S2).

To better visualize the phosphoproteomic data, two types of heatmaps were generated for each peptide using the in-house Peptide Depot software platform.[50] For each cell line, abundance heatmaps visualizing the average phosphopeptide abundances across the time series were created (Figure 1, pictured in a blue/yellow color scale). Additionally, a ratio heatmap visualizing the fold changes in phosphopeptide abundance between Jgamma1 and Jgamma1.WT at each timepoint was also created (Figure 1, pictured in a red/green color scale). As discussed in the Materials and Methods section, stringent statistical testing and multiple hypothesis correction were performed to determine both significant changes in phosphopeptide abundance as a function of time as well as significant changes in phosphopeptide abundance between the two cell lines. The biological conclusions discussed herein are drawn from timepoints with $q < .05$, which are annotated directly on the corresponding heatmap squares with a white dot.

Overall, a total of 1557 unique tyrosine phosphorylation sites from 1012 proteins were identified at less than 1% FDR. The high quality and reproducibility of each LC/MS run were demonstrated by analyzing the pairwise correlation of SIC peak areas observed in separate replicates (average R^2 of 0.83 ± 0.05) (Figure S3).

Analysis of KEGG12Annotated TCR Signaling Proteins

To obtain a more focused view of phosphorylation events occurring on canonical TCR signaling proteins, we examined the subset of sites in our data on proteins included in the Kyoto Encyclopedia of Genes and Genomes (KEGG) T Cell Receptor Signaling Pathway category.[51] In total, 97 unique tyrosine phosphorylation sites on 54 KEGG-annotated TCR signaling pathway proteins were observed. A selection of these sites are displayed in Figure 1, and in the context of the pathway in Figure 2. Abundance heatmaps created for these sites in the Jgamma1.WT line (Figure 1) indicate that induction of TCR signaling proceeds normally in PLC-γ1-reconstituted T cells and with the expected kinetics.

Analysis of Lck Substrates in Jgamma1

Based on previous investigations revealing the existence of multiple feedback pathways connecting canonical T cell signaling proteins back to Lck[26–28, 52], we hypothesized that PLC-γ1 may also influence the upstream kinase's activity via an indirect mechanism. To determine if Lck activity is altered by the loss of PLC-γ1, we performed hierarchical

clustering of known and predicted Lck substrates observed in our dataset (Figure 3). This analysis revealed divergent phosphorylation patterns at Lck substrate sites, with distinct clusters of sites exhibiting constitutively increased and decreased fold-changes in phosphorylation across the timecourse. Among the phosphopeptides derived from CD3 receptor subunits and the TCRζ chain, the majority clustered together due to their decreased abundance in Jgamma1 (Figure 3B, cluster v). In contrast, phosphopeptides exhibiting constitutively elevated abundance in Jgamma1 also clustered together, and notably included a number of sites located on SLP-76-associated proteins (Figure 3B, cluster iv). Together, these results suggest that PLC-γ1 positively regulates phosphorylation of Lck substrates at the TCR while negatively regulating phosphorylation of other Lck substrates.

Discussion

TCR-CD3 ITAM and ZAP-70 Phosphorylation is Positively Regulated by PLC-γ1

Phosphorylation of CD3 and ζ subunit cytoplasmic tails by Lck is among the earliest events in the initiation of TCR signal transduction. Phosphopeptides observed in our data encompass nearly every ITAM tyrosine on the ζ chain as well as ITAM sites on CD3 δ, ε, and γ. The majority of CD3 and ζ ITAM tyrosines exhibited constitutively and significantly decreased phosphorylation in Jgamma1 compared to Jgamma1.WT cells (Figure 1). Notably, phosphorylation of these residues is significantly lower in Jgamma1 at all timepoints, including samples taken prior to pathway activation at 0 minutes. Western blot confirmed that receptor subunit abundance was unchanged between Jgamma1 and Jgamma1.WT (Figure S4). These data indicate that basal phosphorylation of receptor ITAM sites is disrupted in the absence of PLC-γ1, and that this disruption persists through the first 10 minutes of TCR activation. Despite the overall decrease in ITAM phosphorylation in Jgamma1, examination of ITAM phosphorylation kinetics indicates that phosphorylation of these sites is still induced by OKT3 stimulation in both PLC-γ1-deficient and reconstituted cell lines (Figure 4).

TCR Complex Positive Regulation by PLC-γ1

The phosphorylated CD3 ITAMs provide a docking site for the SH2 domains of the Syk family kinase Zap-7, which becomes activated through both autophosphorylation and modification by Lck.[3, 53] Our phosphoproteomic findings revealed decreased phosphorylation of Tyr^{492} and Tyr^{493} of Zap-7, two positive regulatory residues located within the activation loop of the kinase[4, 54–55] at multiple timepoints in Jgamma1, consistent with impaired activation of Zap-7 (Figure 5E–F). Additionally, we noted decreased phosphorylation of Tyr^{319} of Zap-7 in Jgamma1 (Figure 5D). This residue mediates Zap-7 ’s interaction with Lck, and correlates with Zap-7 activity.[56–58] The statistically significant decreases in Tyr^{319} and Tyr^{493} phosphorylation observed in Jgamma1 were verified by Western blot (Figure S5). The decreased phosphorylation of Zap-7 is consistent with the decreased phosphorylation of ITAMs in the PLC-γ1 deficient cells. Lck phosphorylation of ITAM tyrosine residues is critical in T cell signaling.[59–61] Disruption of ITAM tyrosine phosphorylation in PLC-γ1 deficient cells could arise from decreased activation of Lck or mislocalization of the kinase away from substrate ITAMs. Tyr^{505}, a negative regulatory residue on Lck,[62–63] revealed no statistically significant changes in phosphorylation (Figure

5A–C). Conversely, Tyr^{394}, which positively regulates Lck kinase activity,[62, 64] exhibited elevated phosphorylation in Jgamma1 relative to Jgammat1.WT at 3 minutes post-stimulation; however, this increase was short-lived, and was not detected 2 minutes later. Despite this evidence that cellular Lck kinase activity was slightly elevated with PLC-γ1 deficiency, the constitutive and significant decrease in phosphorylation on Lck substrate ITAM sites on ζ and CD3δ, ε, and γ as well as the aforementioned Lck-regulated activation sites on Zap-7 indicates that phosphorylation of canonical Lck substrates is impaired in Jgamma1.

Regulation of Lck Specificity via Lck Tyr^{192}

Of the Lck regulatory tyrosines observed in this study, only Tyr^{192} exhibited persistent and significantly elevated phosphorylation in Jgamma1. Tyr^{192} is located in the SH2 domain of Lck, and regulates the ligand binding selectivity of the domain.[65–66] In its Tyr^{192}-phosphorylated form, Lck demonstrates enhanced association with TSAd as well as Itk and Pyk2,[66–67] both of which exhibited increased phosphorylation in Jgamma1 in our study (Figure 3, cluster iii). Phosphorylation of this site is thought to alter the substrate targeting of Lck by diverting it from its early signaling program, which includes phosphorylation of ITAMs and Zap-7, to a later one involving activation of Itk as well as effectors of negative feedback.[65–66] Lck-deficient JCAM 1.6 cells reconstituted with mutant Lck-Y192F exhibit increased tyrosine phosphorylation on TCRζ and a greater tendency to form clusters of active Lck.[66, 68] Our observation that PLC-γ1 deficiency significantly elevated Tyr^{192} phosphorylation and decreased ITAM and Zap-7 phosphorylation supports a model wherein PLC-γ1 regulates Lck localization through Tyr^{192}.

SLP1276 Signalosome Component Phosphorylation is Negatively Regulated by PLC12γ1

The simultaneous observation of unimpaired Lck activity and significantly decreased phosphorylation of selected Lck substrates suggests a paradoxical outcome of PLC-γ1 deficiency on Lck activity. Yet this apparent paradox was resolved when an examination of proteins within the SLP-76 complex revealed significantly elevated phosphorylation on a multitude of sites, including multiple residues on Itk, Vav1, PLC-γ2, and ADAP (Figure 1, 3B, cluster iii). Although function and upstream kinases have not been definitively established for all the observed sites, all four proteins are known or predicted direct substrates of Lck that associate directly with SLP-76 and exhibit TCR stimulation-dependent phosphorylation.[17, 69–73] Among the multiple Itk tyrosine residues exhibiting significant and constitutive elevated phosphorylation in Jgamma1, the canonical Lck substrate site, Tyr^{512}, is of particular interest (Figure 5G). Tyr^{512} is located within the activation loop of Itk, and phosphorylation of this residue by Lck promotes Itk's kinase activity.[70, 74] Subsequent examination confirmed that Itk abundance was unchanged between Jgamma1 and Jgamma1.WT (Figure S6). In all, these data suggest that in the absence of PLC-γ1, Lck activity is shifted from the TCR to the SLP-76 complex and activation of Itk by Lck is promoted.

Models for PLC12γ1 Regulation of Lck through SLP1276 or TSAd

Reduced ITAM and Zap-7 phosphorylation and increased SLP-76 complex protein phosphorylation could be explained by mislocalization of Lck in PLC-γ1 deficient cells.

Both PLC-γ1 and Lck have been demonstrated to bind SLP-76's proline-rich region in an SH3 domain-dependent fashion.[6, 13, 75–77] However, only PLC-γ1 has been shown to constitutively associate with SLP-76 in resting T cells.[77] In light of the phosphoproteomic data, we speculate that the absence of PLC-γ1 could allow Lck to bind the less occupied proline-rich region on SLP-76, bringing it into proximity with Itk and other SLP-76-scaffolded signaling proteins.[5] Decreased ITAM phosphorylation could thus result from depletion of Lck at the receptor. In support of this model, the Lck SH3 domain was shown previously to impact both Lck substrate selectivity and T cell development in mice using an SH3 inactivating mutant, W97A. Lck W97A mutant mice exhibit impaired early thymocyte development within the CD4+ and CD8+ lineages.[78] Lck substrate specificity was perturbed in Lck W97A thymocytes, with elevated Zap-7 phosphorylation and reduced LAT and PLC-γ1 phosphorylation in response to TCR stimulation.[78] Furthermore, Jurkat cells expressing Lck W97A showed dramatic elevation of TCRζ subunit and Zap-7 Tyr^{319} phosphorylation, opposite the patterns observed in our data (Figure 1).[79] These data indicate that the Lck SH3 domain decreases Lck substrate phosphorylation at the TCR, resulting in elevated SLP-76 complex phosphorylation both *in vitro* and *in vivo*.

Lck substrate specificity within the TCR and SLP-76 complex can also be regulated by the protein T cell specific adaptor (TSAd). Previous studies point to an inverse correlation between TSAd expression and TCRζ phosphorylation, with TSAd-deficient T cells exhibiting increased ζ phosphorylation[66] and TSAd-overexpressing T cells exhibiting decreased ζ phosphorylation.[80] Both Itk and Lck associate with TSAd, and this association is reinforced by Itk's phosphorylation of Tyr^{192} on Lck, which promotes the interaction of Lck's SH2 domain with TSAd.[66] Reciprocally, Lck and TSAd promote phosphorylation of Itk's Tyr^{512} residue, and TSAd is required for robust phosphorylation of Itk in Jurkat cells.[81] Our phosphoproteomic data reveal increased phosphorylation on multiple Itk residues spanning the full duration of the experiment (Figure 1,3). The elevation of phosphorylation at both Lck Tyr^{192} and Itk Tyr^{512} in PLC-γ1 deficient cells suggests that association of these proteins is increased in the absence of PLC-γ1. As a consequence of increased recruitment of Itk and Lck to TSAd, decreased phosphorylation of CD3 and ζ ITAMs may occur as Lck is titrated away from CD3 subunits.

Models proposing sequestration of Lck on SLP-76 or TSAd are not mutually exclusive, as Lck may associate with both adaptors simultaneously via separate Src homology domains.[76, 82] Previous investigations have demonstrated that TSAd also associates directly with Nck, and in turn promotes its association with SLP-76.[83] Like Lck, Nck's associations with SLP-76 and TSAd may also be mediated by separate domains.[83–85] An intriguing possibility that is in agreement with the results of the present study as well as previous findings is that Lck could participate in a multimolecular signaling complex containing both SLP-76 and TSAd, the formation of which occurs only in late TCR signaling under normal conditions.

TCR12 and PLC12γ1-Dependent Phosphorylation of PLC12γ2

Previous studies have suggested PLC-γ2 is capable of partially compensating for the absence of PLC-γ1.[19, 24–25] Our phosphoproteomic data yielded peptides encompassing

three functionally significant PLC-γ2 residues, Tyr^{753}, Tyr^{759}, and Tyr^{1217} (Figure 6). Tyr^{753} and Tyr^{759} are located between the C-terminal SH2 and the SH3 domain of PLC-γ2. Phosphorylation of these residues induces intramolecular associations of PLC-γ2's SH2 domains, forcing the active site of the enzyme into an open conformation.[12] Tyr^{1217} is located in the carboxy-terminal region of PLC-γ2, and like Tyr^{753} and Tyr^{759}, is required for maximal phospholipase activity.[86] While the role of Tec family kinases in regulating Tyr^{753} and Tyr^{759} is well established, regulation of Tyr^{1217} by the Tec family is still subject to debate.[17–18, 86] In both the Jgamma1 and Jgamma1.WT lines, phosphorylation of these sites was induced by TCR stimulation, with Jgamma1 exhibiting significantly more phosphorylation at these residues (Figure 6). These results indicate both that PLC-γ2 is rapidly phosphorylated during early TCR activation and that PLC-γ1 negatively regulates the phosphorylation of PLC-γ2. This regulation may be due to excess PLC-γ1 outcompeting PLC-γ2 for access to the SLP-76 SH3 domain, which situates PLC-γ1 in proximity to Itk. In the absence of PLC-γ1, increased activation of PLC-γ2 may be sufficient to partially compensate for the loss of PLC-γ1's phospholipase activity. Consistent with a previous study of PLCγ1 conditionally deficient mice[23], we did not observe a significant change in the phosphorylation state of Erk's activating residues in Jgamma1. The maintenance of phosphorylation on Erk is likely due to the compensatory effects of PLC-γ2. Our findings in Jurkat cells agreed with observations of PLC-γ1 conditionally deficient mice, which also showed elevated phosphorylation of JNK (Figure 6).[23] Vav1 GEF/Rac recruitment may be heightened in the absence of PLC-γ1 as a result of elevated PIP_3 levels [87–88], which could arise due to both an increase in PIP_2 as well as heightened activation of PI3k, as assessed by the increased phosphorylation of Tyr^{467} of p85α (Figure 1).[89–91] This mechanism has previously been established in T cells,[92] and may involve Pyk2.[93–94] In total, the phosphoproteomic data indicate that Lck targeting but not activity is regulated by PLC-γ1 through an Erk-independent mechanism.

Conclusions

To date, numerous studies have highlighted PLC-γ1's importance in modulating MAPK pathways as well as regulating intracellular Ca^{2+}. However, the role that PLC-γ1 serves in regulating the upstream phosphorylation events that precede cleavage of PIP_2 in activated T cells is not well understood. In this study, we employed a quantitative MS/MS-based strategy to explore dynamic tyrosine phosphorylation in PLC-γ1-deficient T cells. Our results highlight a role for PLC-γ1 in regulating the activity and substrate specificity of Lck. PLC-γ1 may carry out this function by outcompeting Lck for access to SLP-76 and Itk, by promoting the interaction of Lck Tyr^{192} and TSAd, or some combination of both mechanisms (Figure 7). Furthermore, our data reveal that Erk activity is not significantly diminished by the loss of PLC-γ1 during the first 10 minutes of TCR signal transduction, and that this may be due to a buffering effect of PLC-γ2 expressed in T cells. We speculate that increased activation of JNK may occur via Vav1/Rac as a consequence of elevated PIP_3 brought on by the absence of PLC-γ1. In total, our results confirm the central role PLC-γ1 plays in orchestrating the events of early TCR signal transduction, and suggest that PLC-γ1 may exert a significant regulatory influence on feedback pathways connecting the signalosome complex to Lck.

Supplementary Material

Refer to Web version on PubMed Central for supplementary material.

Acknowledgments

Acknowledgements and Funding

We acknowledge financial support from NIH grants R01AI083636 (A.R.S) and T32GM007601 (J.B.). Research reported in this publication was supported by the Proteomics Core of the COBRE Center for Cancer Research Development, funded by the National Institute of General Medical Sciences of the National Institutes of Health under Award Number P30GM110759. This research is based in part upon work conducted using the Rhode Island NSF/EPSCoR Proteomics Shared Resource Facility, which is supported in part by the National Science Foundation EPSCoR Grant No. 1004057, National Institutes of Health Grant No. 1S10RR020923, a Rhode Island Science and Technology Advisory Council grant and the Division of Biology and Medicine, Brown University.

References

1. Salmond RJ, Filby A, Qureshi I, Caserta S, Zamoyska R. T-cell receptor proximal signaling via the Src-family kinases, Lck and Fyn, influences T-cell activation, differentiation, and tolerance. Immunol Rev. 2009; 228(1):9–22. [PubMed: 19290918]
2. Chan AC, Dalton M, Johnson R, Kong GH, Wang T, Thoma R, Kurosaki T. Activation of ZAP-70 kinase activity by phosphorylation of tyrosine 493 is required for lymphocyte antigen receptor function. EMBO J. 1995; 14(11):2499–508. [PubMed: 7781602]
3. Neumeister EN, Zhu Y, Richard S, Terhorst C, Chan AC, Shaw AS. Binding of ZAP-70 to phosphorylated T-cell receptor zeta and eta enhances its autophosphorylation and generates specific binding sites for SH2 domain-containing proteins. Mol Cell Biol. 1995; 15(6):3171–8. [PubMed: 7760813]
4. Kong G, Dalton M, Bubeck Wardenburg J, Straus D, Kurosaki T, Chan AC. Distinct tyrosine phosphorylation sites in ZAP-70 mediate activation and negative regulation of antigen receptor function. Mol Cell Biol. 1996; 16(9):5026–35. [PubMed: 8756661]
5. Koretzky GA, Abtahian F, Silverman MA. SLP76 and SLP65: complex regulation of signalling in lymphocytes and beyond. Nat Rev Immunol. 2006; 6(1):67–78. [PubMed: 16493428]
6. Yablonski D, Kuhne MR, Kadlecek T, Weiss A. Uncoupling of nonreceptor tyrosine kinases from PLC-gamma1 in an SLP-76-deficient T cell. Science. 1998; 281(5375):413–6. [PubMed: 9665884]
7. Su YW, Zhang Y, Schweikert J, Koretzky GA, Reth M, Wienands J. Interaction of SLP adaptors with the SH2 domain of Tec family kinases. Eur J Immunol. 1999; 29(11):3702–11. [PubMed: 10556826]
8. Bubeck Wardenburg J, Fu C, Jackman JK, Flotow H, Wilkinson SE, Williams DH, Johnson R, Kong G, Chan AC, Findell PR. Phosphorylation of SLP-76 by the ZAP-70 protein-tyrosine kinase is required for T-cell receptor function. J Biol Chem. 1996; 271(33):19641–4. [PubMed: 8702662]
9. Kumar L, Pivniouk V, de la Fuente MA, Laouini D, Geha RS. Differential role of SLP-76 domains in T cell development and function. Proc Natl Acad Sci U S A. 2002; 99(2):884–9. [PubMed: 11792851]
10. Kadamur G, Ross EM. Mammalian phospholipase C. Annu Rev Physiol. 2013; 75:127–54. [PubMed: 23140367]
11. Yang YR, Choi JH, Chang JS, Kwon HM, Jang HJ, Ryu SH, Suh PG. Diverse cellular and physiological roles of phospholipase C-gamma1. Adv Biol Regul. 2012; 52(1):138–51. [PubMed: 21964416]
12. Gresset A, Hicks SN, Harden TK, Sondek J. Mechanism of phosphorylation-induced activation of phospholipase C-gamma isozymes. J Biol Chem. 2010; 285(46):35836–47. [PubMed: 20807769]
13. Yablonski D, Kadlecek T, Weiss A. Identification of a phospholipase C-gamma1 (PLC-gamma1) SH3 domain-binding site in SLP-76 required for T-cell receptor-mediated activation of PLC-gamma1 and NFAT. Mol Cell Biol. 2001; 21(13):4208–18. [PubMed: 11390650]

14. Irvin BJ, Williams BL, Nilson AE, Maynor HO, Abraham RT. Pleiotropic contributions of phospholipase C-gamma1 (PLC-gamma1) to T-cell antigen receptor-mediated signaling: reconstitution studies of a PLC-gamma1-deficient Jurkat T-cell line. Mol Cell Biol. 2000; 20(24): 9149–61. [PubMed: 11094067]
15. Stoica B, DeBell KE, Graham L, Rellahan BL, Alava MA, Laborda J, Bonvini E. The amino-terminal Src homology 2 domain of phospholipase C gamma 1 is essential for TCR-induced tyrosine phosphorylation of phospholipase C gamma 1. J Immunol. 1998; 160(3):1059–66. [PubMed: 9570517]
16. Falasca M, Logan SK, Lehto VP, Baccante G, Lemmon MA, Schlessinger J. Activation of phospholipase C gamma by PI 3-kinase-induced PH domain-mediated membrane targeting. EMBO J. 1998; 17(2):414–22. [PubMed: 9430633]
17. Humphries LA, Dangelmaier C, Sommer K, Kipp K, Kato RM, Griffith N, Bakman I, Turk CW, Daniel JL, Rawlings DJ. Tec kinases mediate sustained calcium influx via site-specific tyrosine phosphorylation of the phospholipase Cgamma Src homology 2-Src homology 3 linker. J Biol Chem. 2004; 279(36):37651–61. [PubMed: 15184383]
18. Ozdener F, Dangelmaier C, Ashby B, Kunapuli SP, Daniel JL. Activation of phospholipase Cgamma2 by tyrosine phosphorylation. Mol Pharmacol. 2002; 62(3):672–9. [PubMed: 12181444]
19. Fu G, Chen Y, Schuman J, Wang D, Wen R. Phospholipase Cgamma2 plays a role in TCR signal transduction and T cell selection. J Immunol. 2012; 189(5):2326–32. [PubMed: 22837484]
20. Thomas SM, Coppelli FM, Wells A, Gooding WE, Song J, Kassis J, Drenning SD, Grandis JR. Epidermal growth factor receptor-stimulated activation of phospholipase Cgamma-1 promotes invasion of head and neck squamous cell carcinoma. Cancer Res. 2003; 63(17):5629–35. [PubMed: 14500405]
21. Sala G, Dituri F, Raimondi C, Previdi S, Maffucci T, Mazzoletti M, Rossi C, Iezzi M, Lattanzio R, Piantelli M, Iacobelli S, Broggini M, Falasca M. Phospholipase Cgamma1 is required for metastasis development and progression. Cancer Res. 2008; 68(24):10187–96. [PubMed: 19074886]
22. Jones NP, Katan M. Role of phospholipase Cgamma1 in cell spreading requires association with a beta-Pix/GIT1-containing complex, leading to activation of Cdc42 and Rac1. Mol Cell Biol. 2007; 27(16):5790–805. [PubMed: 17562871]
23. Fu G, Chen Y, Yu M, Podd A, Schuman J, He Y, Di L, Yassai M, Haribhai D, North PE, Gorski J, Williams CB, Wang D, Wen R. Phospholipase C{gamma}1 is essential for T cell development, activation, and tolerance. J Exp Med. 2010; 207(2):309–18. [PubMed: 20123962]
24. Wen R, Chen Y, Schuman J, Fu G, Yang S, Zhang W, Newman DK, Wang D. An important role of phospholipase Cgamma1 in pre-B-cell development and allelic exclusion. EMBO J. 2004; 23(20): 4007–17. [PubMed: 15372077]
25. Coggeshall KM, McHugh JC, Altman A. Predominant expression and activation-induced tyrosine phosphorylation of phospholipase C-gamma 2 in B lymphocytes. Proc Natl Acad Sci U S A. 1992; 89(12):5660–4. [PubMed: 1376928]
26. Cao L, Ding Y, Hung N, Yu K, Ritz A, Raphael BJ, Salomon AR. Quantitative phosphoproteomics reveals SLP-76 dependent regulation of PAG and Src family kinases in T cells. PLoS One. 2012; 7(10):e46725. [PubMed: 23071622]
27. Sjolin-Goodfellow H, Frushicheva MP, Ji Q, Cheng DA, Kadlecek TA, Cantor AJ, Kuriyan J, Chakraborty AK, Salomon AR, Weiss A. The catalytic activity of the kinase ZAP-70 mediates basal signaling and negative feedback of the T cell receptor pathway. Sci Signal. 2015; 8(377):ra49. [PubMed: 25990959]
28. Helou YA, Petrashen AP, Salomon AR. Vav1 Regulates T-Cell Activation through a Feedback Mechanism and Crosstalk between the T-Cell Receptor and CD28. J Proteome Res. 2015
29. Salomon AR, Ficarro SB, Brill LM, Brinker A, Phung QT, Ericson C, Sauer K, Brock A, Horn DM, Schultz PG, Peters EC. Profiling of tyrosine phosphorylation pathways in human cells using mass spectrometry. Proc Natl Acad Sci U S A. 2003; 100(2):443–8. [PubMed: 12522270]
30. Ji Q, Ding Y, Salomon AR. SRC homology 2 domain-containing leukocyte phosphoprotein of 76 kDa (SLP-76) N-terminal tyrosine residues regulate a dynamic signaling equilibrium involving

feedback of proximal T-cell receptor (TCR) signaling. Mol Cell Proteomics. 2015; 14(1):30–40. [PubMed: 25316710]

31. Rappsilber J, Ishihama Y, Mann M. Stop and go extraction tips for matrix-assisted laser desorption/ionization, nanoelectrospray, and LC/MS sample pretreatment in proteomics. Analytical Chemistry. 2003; 75(3):663–670. [PubMed: 12585499]
32. Ficarro SB, Salomon AR, Brill LM, Mason DE, Stettler-Gill M, Brock A, Peters EC. Automated immobilized metal affinity chromatography/nano-liquid chromatography/electrospray ionization mass spectrometry platform for profiling protein phosphorylation sites. Rapid Commun Mass Spectrom. 2005; 19(1):57–71. [PubMed: 15570572]
33. Licklider LJ, Thoreen CC, Peng J, Gygi SP. Automation of nanoscale microcapillary liquid chromatography-tandem mass spectrometry with a vented column. Anal Chem. 2002; 74(13): 3076–83. [PubMed: 12141667]
34. Ahsan N, Salomon AR. Quantitative Phosphoproteomic Analysis of T-Cell Receptor Signaling. Methods Mol Biol. 2017; 1584:369–382. [PubMed: 28255713]
35. Yu K, Sabelli A, DeKeukelaere L, Park R, Sindi S, Gatsonis CA, Salomon A. Integrated platform for manual and high-throughput statistical validation of tandem mass spectra. Proteomics. 2009; 9(11):3115–25. [PubMed: 19526561]
36. Yu K, Salomon AR. HTAPP: high-throughput autonomous proteomic pipeline. Proteomics. 2010; 10(11):2113–22. [PubMed: 20336676]
37. Perkins DN, Pappin DJC, Creasy DM, Cottrell JS. Probability-based protein identification by searching sequence databases using mass spectrometry data. Electrophoresis. 1999; 20(18):3551–3567. [PubMed: 10612281]
38. Elias JE, Gygi SP. Target-decoy search strategy for increased confidence in large-scale protein identifications by mass spectrometry. Nat Methods. 2007; 4(3):207–14. [PubMed: 17327847]
39. Beausoleil SA, Villen J, Gerber SA, Rush J, Gygi SP. A probability-based approach for high-throughput protein phosphorylation analysis and site localization. Nat Biotechnol. 2006; 24(10): 1285–92. [PubMed: 16964243]
40. Demirkan G, Yu K, Boylan JM, Salomon AR, Gruppuso PA. Phosphoproteomic profiling of in vivo signaling in liver by the mammalian target of rapamycin complex 1 (mTORC1). PLoS One. 2011; 6(6):e21729. [PubMed: 21738781]
41. Nguyen V, Cao L, Lin JT, Hung N, Ritz A, Yu K, Jianu R, Ulin SP, Raphael BJ, Laidlaw DH, Brossay L, Salomon AR. A new approach for quantitative phosphoproteomic dissection of signaling pathways applied to T cell receptor activation. Mol Cell Proteomics. 2009; 8(11):2418–31. [PubMed: 19605366]
42. Storey JD. The positive false discovery rate: A Bayesian interpretation and the q-value. Annals of Statistics. 2003; 31(6):2013–2035.
43. Storey JD, Tibshirani R. Statistical significance for genomewide studies. Proc Natl Acad Sci U S A. 2003; 100(16):9440–5. [PubMed: 12883005]
44. de Hoon MJ, Imoto S, Nolan J, Miyano S. Open source clustering software. Bioinformatics. 2004; 20(9):1453–4. [PubMed: 14871861]
45. Saldanha AJ. Java Treeview--extensible visualization of microarray data. Bioinformatics. 2004; 20(17):3246–8. [PubMed: 15180930]
46. Hornbeck PV, Zhang B, Murray B, Kornhauser JM, Latham V, Skrzypek E. PhosphoSitePlus, 2014: mutations, PTMs and recalibrations. Nucleic Acids Res. 2015; 43(Database issue):D512–20. [PubMed: 25514926]
47. Obenauer JC, Cantley LC, Yaffe MB. Scansite 2.0: Proteome-wide prediction of cell signaling interactions using short sequence motifs. Nucleic Acids Res. 2003; 31(13):3635–41. [PubMed: 12824383]
48. Vizcaino JA, Deutsch EW, Wang R, Csordas A, Reisinger F, Rios D, Dianes JA, Sun Z, Farrah T, Bandeira N, Binz PA, Xenarios I, Eisenacher M, Mayer G, Gatto L, Campos A, Chalkley RJ, Kraus HJ, Albar JP, Martinez-Bartolome S, Apweiler R, Omenn GS, Martens L, Jones AR, Hermjakob H. ProteomeXchange provides globally coordinated proteomics data submission and dissemination. Nat Biotechnol. 2014; 32(3):223–6. [PubMed: 24727771]

49. Vizcaino JA, Csordas A, del-Toro N, Dianes JA, Griss J, Lavidas I, Mayer G, Perez-Riverol Y, Reisinger F, Ternent T, Xu QW, Wang R, Hermjakob H. 2016 update of the PRIDE database and its related tools. Nucleic Acids Res. 2016; 44(D1):D447–56. [PubMed: 26527722]
50. Yu K, Salomon AR. PeptideDepot: flexible relational database for visual analysis of quantitative proteomic data and integration of existing protein information. Proteomics. 2009; 9(23):5350–8. [PubMed: 19834895]
51. Kanehisa M. The KEGG database. Novartis Found Symp. 2002; 247:91–101. discussion 101–3, 119–28, 244–52. [PubMed: 12539951]
52. Helou YA, Nguyen V, Beik SP, Salomon AR. ERK positive feedback regulates a widespread network of tyrosine phosphorylation sites across canonical T cell signaling and actin cytoskeletal proteins in Jurkat T cells. PLoS One. 2013; 8(7):e69641. [PubMed: 23874979]
53. Wange RL, Guitian R, Isakov N, Watts JD, Aebersold R, Samelson LE. Activating and inhibitory mutations in adjacent tyrosines in the kinase domain of ZAP-70. J Biol Chem. 1995; 270(32): 18730–3. [PubMed: 7642520]
54. Watts JD, Affolter M, Krebs DL, Wange RL, Samelson LE, Aebersold R. Identification by electrospray ionization mass spectrometry of the sites of tyrosine phosphorylation induced in activated Jurkat T cells on the protein tyrosine kinase ZAP-70. J Biol Chem. 1994; 269(47): 29520–9. [PubMed: 7961936]
55. Mege D, Di Bartolo V, Germain V, Tuosto L, Michel F, Acuto O. Mutation of tyrosines 492/493 in the kinase domain of ZAP-70 affects multiple T-cell receptor signaling pathways. J Biol Chem. 1996; 271(51):32644–52. [PubMed: 8955094]
56. Di Bartolo V, Mege D, Germain V, Pelosi M, Dufour E, Michel F, Magistrelli G, Isacchi A, Acuto O. Tyrosine 319, a newly identified phosphorylation site of ZAP-70, plays a critical role in T cell antigen receptor signaling. J Biol Chem. 1999; 274(10):6285–94. [PubMed: 10037717]
57. Pelosi M, Di Bartolo V, Mounier V, Mege D, Pascussi JM, Dufour E, Blondel A, Acuto O. Tyrosine 319 in the interdomain B of ZAP-70 is a binding site for the Src homology 2 domain of Lck. J Biol Chem. 1999; 274(20):14229–37. [PubMed: 10318843]
58. Williams BL, Irvin BJ, Sutor SL, Chini CC, Yacyshyn E, Bubeck Wardenburg J, Dalton M, Chan AC, Abraham RT. Phosphorylation of Tyr319 in ZAP-70 is required for T-cell antigen receptor-dependent phospholipase C-gamma1 and Ras activation. EMBO J. 1999; 18(7):1832–44. [PubMed: 10202147]
59. Straus DB, Weiss A. Genetic evidence for the involvement of the lck tyrosine kinase in signal transduction through the T cell antigen receptor. Cell. 1992; 70(4):585–93. [PubMed: 1505025]
60. van Oers NS, Killeen N, Weiss A. Lck regulates the tyrosine phosphorylation of the T cell receptor subunits and ZAP-70 in murine thymocytes. J Exp Med. 1996; 183(3):1053–62. [PubMed: 8642247]
61. Wong J, Straus D, Chan AC. Genetic evidence of a role for Lck in T-cell receptor function independent or downstream of ZAP-70/Syk protein tyrosine kinases. Mol Cell Biol. 1998; 18(5): 2855–66. [PubMed: 9566904]
62. Palacios EH, Weiss A. Function of the Src-family kinases, Lck and Fyn, in T-cell development and activation. Oncogene. 2004; 23(48):7990–8000. [PubMed: 15489916]
63. Bergman M, Mustelin T, Oetken C, Partanen J, Flint NA, Amrein KE, Autero M, Burn P, Alitalo K. The human p50csk tyrosine kinase phosphorylates p56lck at Tyr-505 and down regulates its catalytic activity. EMBO J. 1992; 11(8):2919–24. [PubMed: 1639064]
64. Abraham N, Veillette A. Activation of p56lck through mutation of a regulatory carboxy-terminal tyrosine residue requires intact sites of autophosphorylation and myristylation. Mol Cell Biol. 1990; 10(10):5197–206. [PubMed: 1697929]
65. Couture C, Songyang Z, Jascur T, Williams S, Tailor P, Cantley LC, Mustelin T. Regulation of the Lck SH2 domain by tyrosine phosphorylation. J Biol Chem. 1996; 271(40):24880–4. [PubMed: 8798764]
66. Granum S, Sundvold-Gjerstad V, Gopalakrishnan RP, Berge T, Koll L, Abrahamsen G, Sorlie M, Spurkland A. The kinase Itk and the adaptor TSAd change the specificity of the kinase Lck in T cells by promoting the phosphorylation of Tyr192. Sci Signal. 2014; 7(355):ra118. [PubMed: 25492967]

67. Berg NN, Ostergaard HL. T cell receptor engagement induces tyrosine phosphorylation of FAK and Pyk2 and their association with Lck. J Immunol. 1997; 159(4):1753–7. [PubMed: 9257837]
68. Kapoor-Kaushik N, Hinde E, Compeer EB, Yamamoto Y, Kraus F, Yang Z, Lou J, Pageon SV, Tabarin T, Gaus K, Rossy J. Distinct Mechanisms Regulate Lck Spatial Organization in Activated T Cells. Front Immunol. 2016; 7:83. [PubMed: 27014263]
69. da Silva AJ, Li Z, de Vera C, Canto E, Findell P, Rudd CE. Cloning of a novel T-cell protein FYB that binds FYN and SH2-domain-containing leukocyte protein 76 and modulates interleukin 2 production. Proc Natl Acad Sci U S A. 1997; 94(14):7493–8. [PubMed: 9207119]
70. Heyeck SD, Wilcox HM, Bunnell SC, Berg LJ. Lck phosphorylates the activation loop tyrosine of the Itk kinase domain and activates Itk kinase activity. J Biol Chem. 1997; 272(40):25401–8. [PubMed: 9312162]
71. Han J, Das B, Wei W, Van Aelst L, Mosteller RD, Khosravi-Far R, Westwick JK, Der CJ, Broek D. Lck regulates Vav activation of members of the Rho family of GTPases. Mol Cell Biol. 1997; 17(3):1346–53. [PubMed: 9032261]
72. Gulbins E, Coggeshall KM, Baier G, Katzav S, Burn P, Altman A. Tyrosine kinase-stimulated guanine nucleotide exchange activity of Vav in T cell activation. Science. 1993; 260(5109):822–5. [PubMed: 8484124]
73. Rodriguez R, Matsuda M, Perisic O, Bravo J, Paul A, Jones NP, Light Y, Swann K, Williams RL, Katan M. Tyrosine residues in phospholipase Cgamma 2 essential for the enzyme function in B-cell signaling. J Biol Chem. 2001; 276(51):47982–92. [PubMed: 11606584]
74. Berg LJ, Finkelstein LD, Lucas JA, Schwartzberg PL. Tec family kinases in T lymphocyte development and function. Annu Rev Immunol. 2005; 23:549–600. [PubMed: 15771581]
75. Gonen R, Beach D, Ainey C, Yablonski D. T cell receptor-induced activation of phospholipase C-gamma1 depends on a sequence-independent function of the P-I region of SLP-76. J Biol Chem. 2005; 280(9):8364–70. [PubMed: 15623534]
76. Sanzenbacher R, Kabelitz D, Janssen O. SLP-76 binding to p56lck: a role for SLP-76 in CD4-induced desensitization of the TCR/CD3 signaling complex. J Immunol. 1999; 163(6):3143–52. [PubMed: 10477581]
77. Jung SH, Jeong JH, Seul HJ, Lee JR. Competition between SLP76 and LAT for PLCgamma1 binding in resting T cells. Eur J Immunol. 2010; 40(8):2330–9. [PubMed: 20544725]
78. Rudd ML, Tua-Smith A, Straus DB. Lck SH3 domain function is required for T-cell receptor signals regulating thymocyte development. Mol Cell Biol. 2006; 26(21):7892–900. [PubMed: 16923964]
79. Li M, Ong SS, Rajwa B, Thieu VT, Geahlen RL, Harrison ML. The SH3 domain of Lck modulates T-cell receptor-dependent activation of extracellular signal-regulated kinase through activation of Raf-1. Mol Cell Biol. 2008; 28(2):630–41. [PubMed: 17998336]
80. Sundvold V, Torgersen KM, Post NH, Marti F, King PD, Rottingen JA, Spurkland A, Lea T. T cell-specific adapter protein inhibits T cell activation by modulating Lck activity. J Immunol. 2000; 165(6):2927–31. [PubMed: 10975797]
81. Berge T, Sundvold-Gjerstad V, Granum S, Andersen TC, Holthe GB, Claesson-Welsh L, Andreotti AH, Inngjerdingen M, Spurkland A. T cell specific adapter protein (TSAd) interacts with Tec kinase ITK to promote CXCL12 induced migration of human and murine T cells. PLoS One. 2010; 5(3):e9761. [PubMed: 20305788]
82. Granum S, Andersen TC, Sorlie M, Jorgensen M, Koll L, Berge T, Lea T, Fleckenstein B, Spurkland A, Sundvold-Gjerstad V. Modulation of Lck function through multisite docking to T cell-specific adapter protein. J Biol Chem. 2008; 283(32):21909–19. [PubMed: 18541536]
83. Hem CD, Sundvold-Gjerstad V, Granum S, Koll L, Abrahamsen G, Buday L, Spurkland A. T cell specific adaptor protein (TSAd) promotes interaction of Nck with Lck and SLP-76 in T cells. Cell Commun Signal. 2015; 13:31. [PubMed: 26163016]
84. Lettau M, Pieper J, Janssen O. Nck adapter proteins: functional versatility in T cells. Cell Commun Signal. 2009; 7:1. [PubMed: 19187548]
85. Wunderlich L, Farago A, Downward J, Buday L. Association of Nck with tyrosine-phosphorylated SLP-76 in activated T lymphocytes. Eur J Immunol. 1999; 29(4):1068–75. [PubMed: 10229072]

86. Watanabe D, Hashimoto S, Ishiai M, Matsushita M, Baba Y, Kishimoto T, Kurosaki T, Tsukada S. Four tyrosine residues in phospholipase C-gamma 2, identified as Btk-dependent phosphorylation sites, are required for B cell antigen receptor-coupled calcium signaling. J Biol Chem. 2001; 276(42):38595–601. [PubMed: 11507089]

87. Han J, Luby-Phelps K, Das B, Shu X, Xia Y, Mosteller RD, Krishna UM, Falck JR, White MA, Broek D. Role of substrates and products of PI 3-kinase in regulating activation of Rac-related guanosine triphosphatases by Vav. Science. 1998; 279(5350):558–60. [PubMed: 9438848]

88. Das B, Shu X, Day GJ, Han J, Krishna UM, Falck JR, Broek D. Control of intramolecular interactions between the pleckstrin homology and Dbl homology domains of Vav and Sos1 regulates Rac binding. J Biol Chem. 2000; 275(20):15074–81. [PubMed: 10748082]

89. Lau C, Wang X, Song L, North M, Wiehler S, Proud D, Chow CW. Syk associates with clathrin and mediates phosphatidylinositol 3-kinase activation during human rhinovirus internalization. J Immunol. 2008; 180(2):870–80. [PubMed: 18178826]

90. Warfel NA, Niederst M, Newton AC. Disruption of the interface between the pleckstrin homology (PH) and kinase domains of Akt protein is sufficient for hydrophobic motif site phosphorylation in the absence of mTORC2. J Biol Chem. 2011; 286(45):39122–9. [PubMed: 21908613]

91. Kim JH, Xu C, Keum YS, Reddy B, Conney A, Kong AN. Inhibition of EGFR signaling in human prostate cancer PC-3 cells by combination treatment with beta-phenylethyl isothiocyanate and curcumin. Carcinogenesis. 2006; 27(3):475–82. [PubMed: 16299382]

92. Turner M, Billadeau DD. VAV proteins as signal integrators for multi-subunit immune-recognition receptors. Nat Rev Immunol. 2002; 2(7):476–86. [PubMed: 12094222]

93. Collins M, Tremblay M, Chapman N, Curtiss M, Rothman PB, Houtman JC. The T cell receptor-mediated phosphorylation of Pyk2 tyrosines 402 and 580 occurs via a distinct mechanism than other receptor systems. J Leukoc Biol. 2010; 87(4):691–701. [PubMed: 20028775]

94. Gao C, Blystone SD. A Pyk2-Vav1 complex is recruited to beta3-adhesion sites to initiate Rho activation. Biochem J. 2009; 420(1):49–56. [PubMed: 19207108]

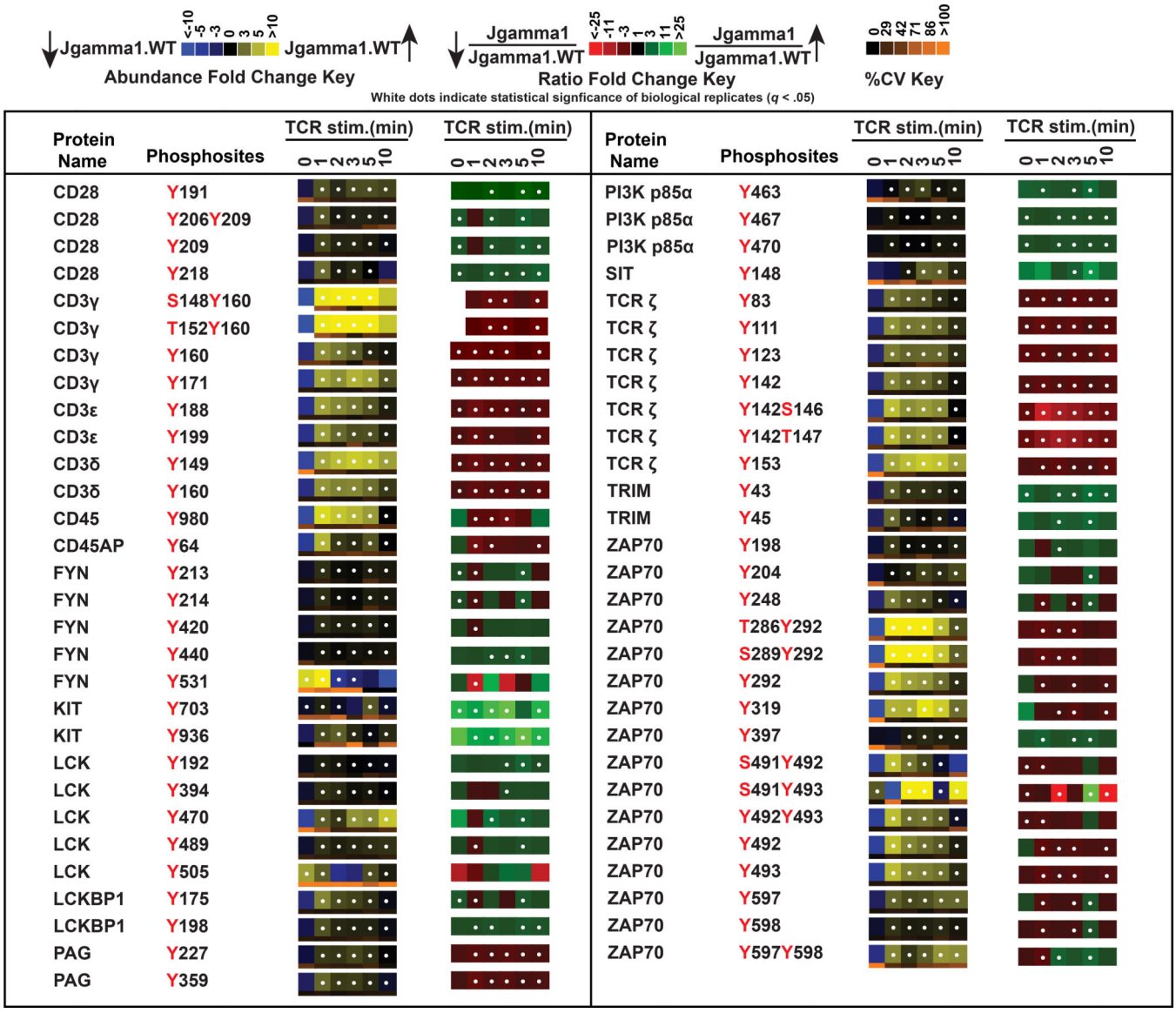

Figure 1.

Quantitative phosphoproteomic analysis of receptor-proximal TCR signaling proteins. Heatmaps were calculated from five biological replicate experiments. Blue/yellow heatmaps represent temporal changes in phosphopeptide abundance in either the Jurkat PLC-γ1 null cell line (Jgamma1) or reconstituted cell line (Jgamma1.WT) following TCR stimulation. Black squares represent a phosphopeptide abundance equal to the geometric mean for that phosphopeptide across all time points for each cell line. Yellow and blue represent phosphopeptide abundances above and below the average, respectively. White dots in the yellow/blue heatmap squares indicate a statistically significant ($q < 0.05$) difference between the phosphopeptide abundance at the indicated timepoint and the lowest abundance of that peptide observed in the time course for that cell line. For each timepoint in which a sufficient number of replicate measurements were observed, the coefficient of variation (CV) was computed. The magnitude of the CV is indicated by the black/orange heatmap

underneath each time point. Red/green heatmaps indicate the ratio between the peptide abundances measured in Jgamma1 and Jgamma1.WT cells for each phosphopeptide at each time point. Black signifies no difference in peptide abundance between the cell lines, while red and green represent reduced and elevated phosphopeptide levels in Jgamma1 relative to Jgamma1.WT, respectively. White dots on red/green ratio heatmap squares indicate a statistically significant difference ($q < 0.05$) in the comparison between Jgamma1 cells and Jgamma1.WT cells ratios for that time point.

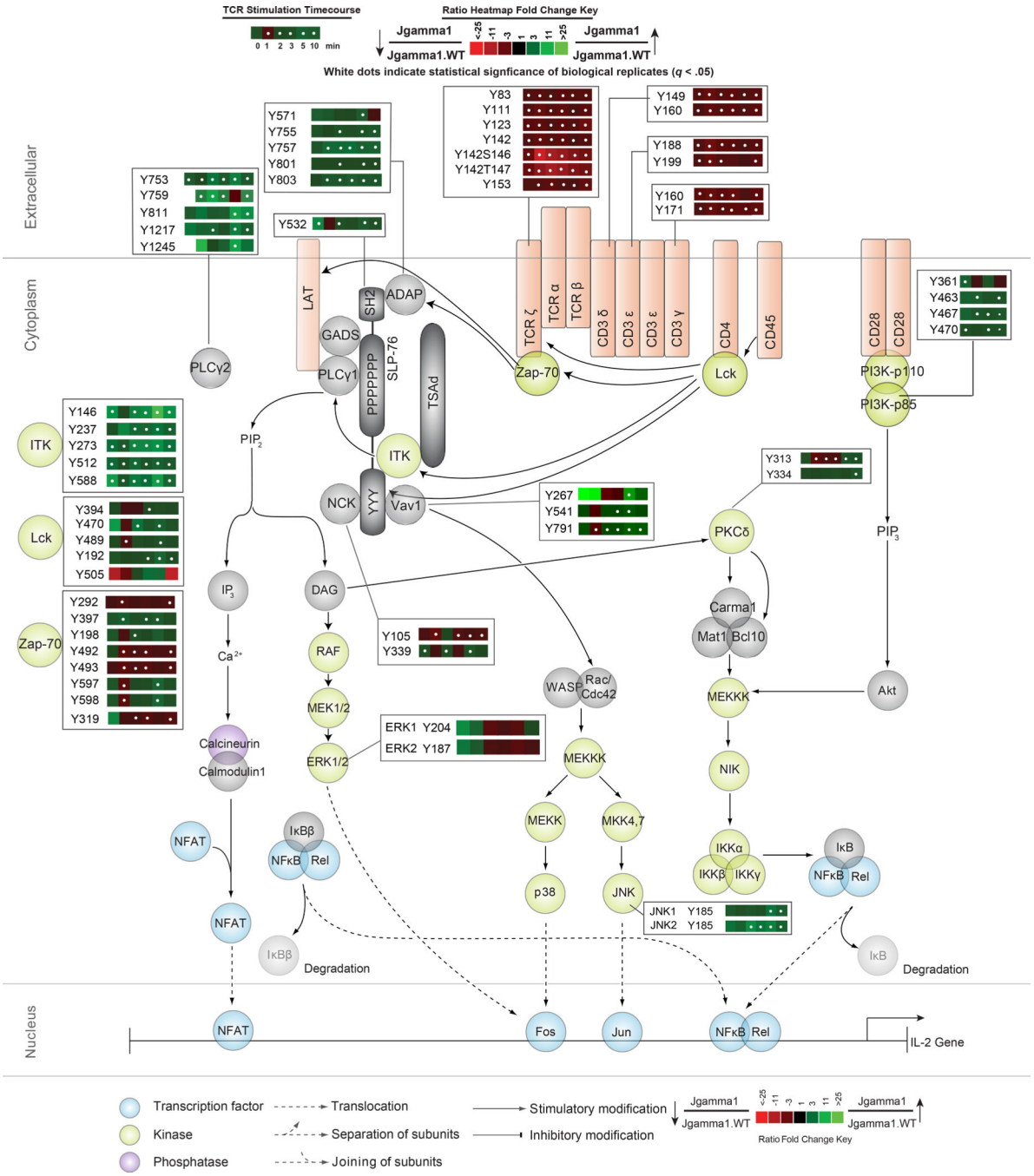

Figure 2.

PLC-γ1 deficiency perturbs phosphorylation on canonical TCR signaling proteins. The canonical TCR signaling pathway is depicted, along with quantitative Jgamma1 to Jgamma1.WT ratio heatmaps depicting altered phosphorylation profiles of select sites. The interpretation of the heatmap color scheme as well as the white dots is the same as that described in Materials and Methods and Figure 1.

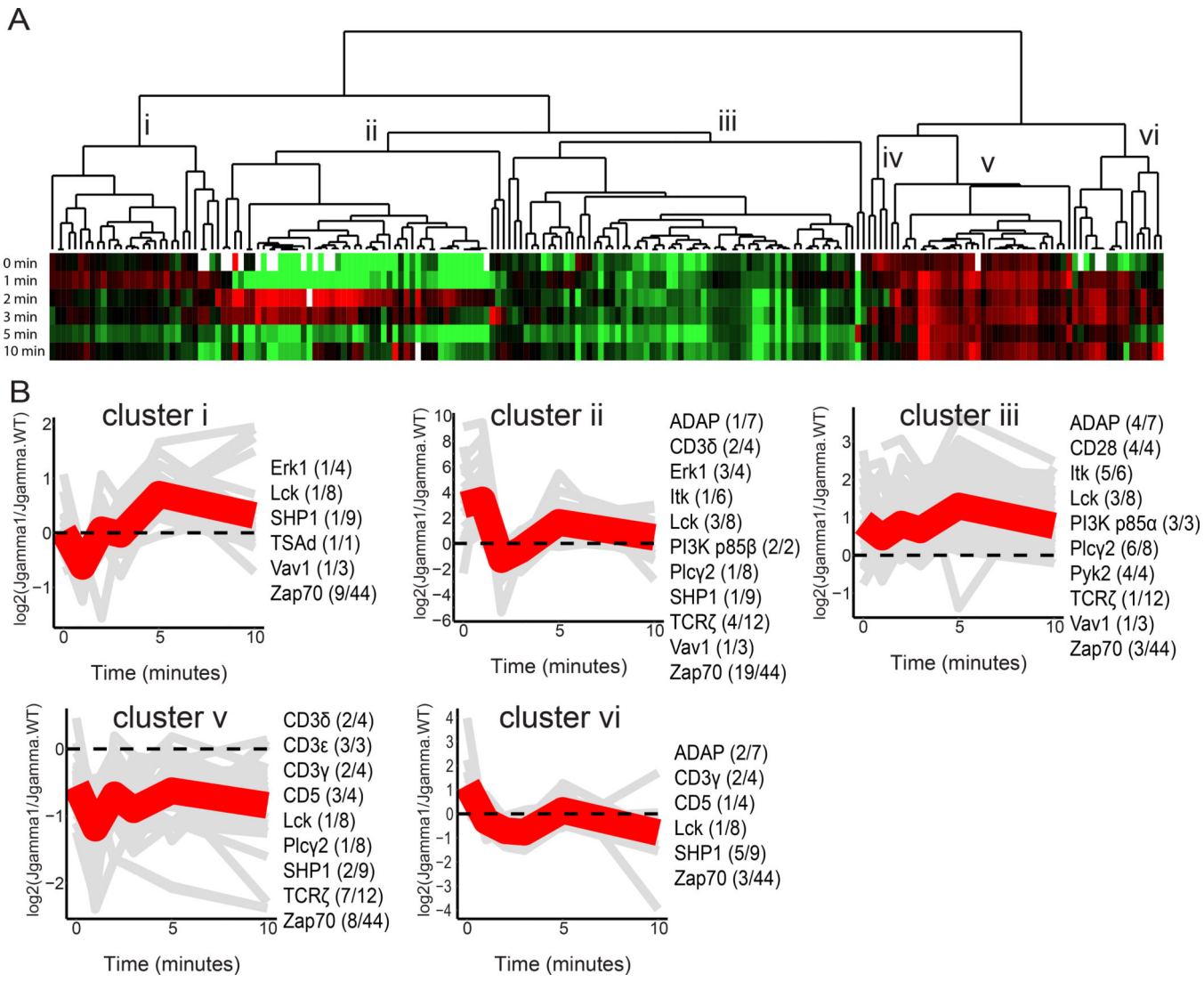

Figure 3.

Hierarchical clustering of known and predicted Lck substrates reveals PLC-γ1-dependent programs of phosphorylation. A) Clustered heatmap of phosphopeptide abundance ratios. The clustered data consists of 195 phosphopeptides in the data derived from proteins that are known or confidently predicted Lck substrates (see Materials and Methods for details). For each peptide selected, the ratios of Jgamma1.WT to Jgamma1 abundance at each timepoint were log2 transformed. Hierarchical clustering was performed using Pearson correlation coefficient as the distance metric and average linkage to calculate cluster distances. B) Time series ratios of phosphopeptides in the five largest clusters obtained. Each plot represents the time course of ratios for each peptide in the cluster (grey series) as well as the population average for the cluster (red series). The text to the right of each plot lists the KEGG-annotated T cell receptor signaling pathway components represented in the cluster, and the proportion of total phosphopeptides of each protein observed in the cluster.

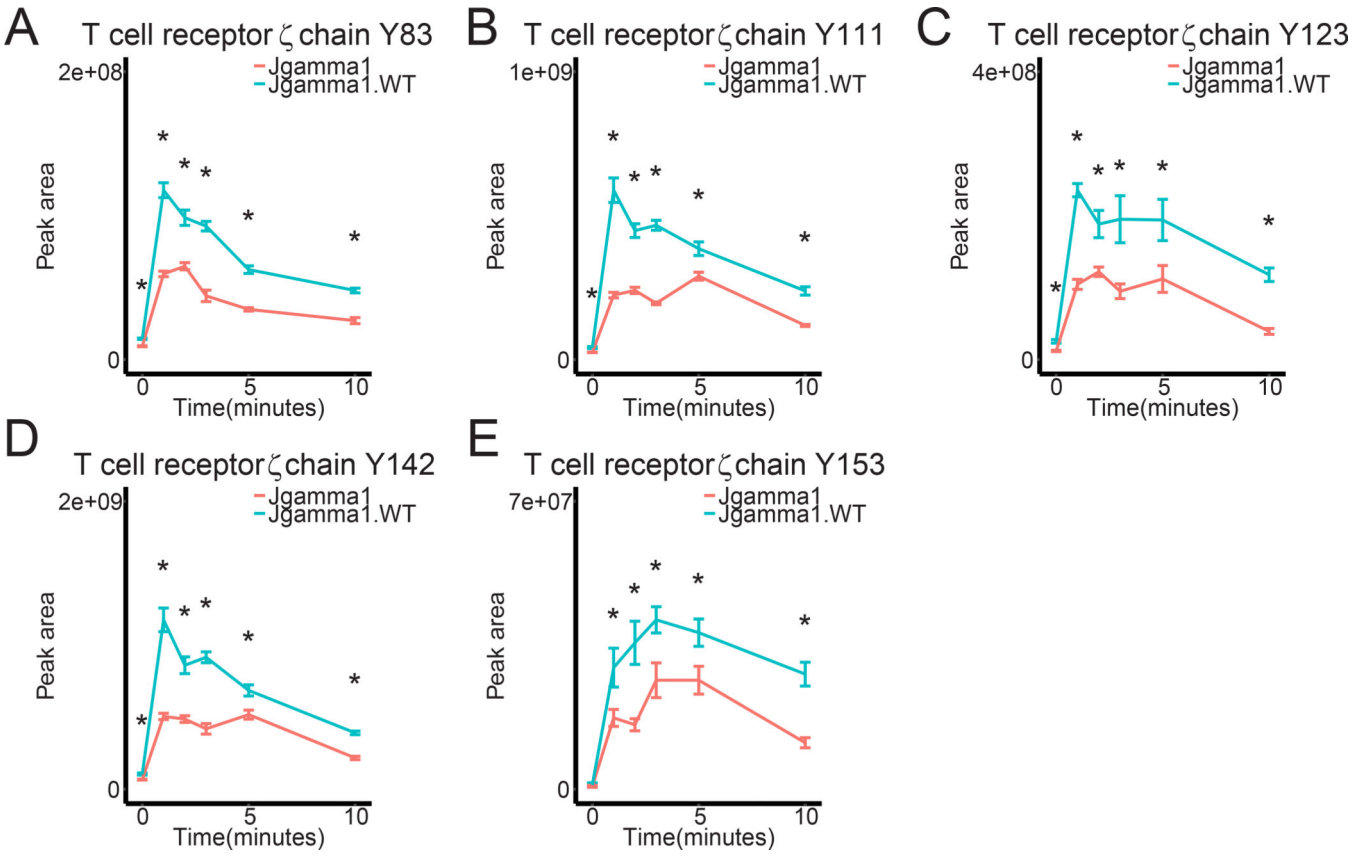

Figure 4.

Phosphorylation kinetics of tyrosine residues located on the T cell receptor ζ chain. Phosphorylation kinetics of TCRζ tyrosines A) Tyr^{83}, B) Tyr^{111}, C) Tyr^{123}, D) Tyr^{142}, and E) Tyr^{153} are depicted during early TCR signaling. Each data point represents the mean phosphopeptide abundance measured across five biological replicate experiments, and error bars indicate the standard error of the mean. Asterisks represent a statistically significant difference ($q < 0.05$) between Jgamma1 cells and Jgamma1.WT cells at the indicated time point.

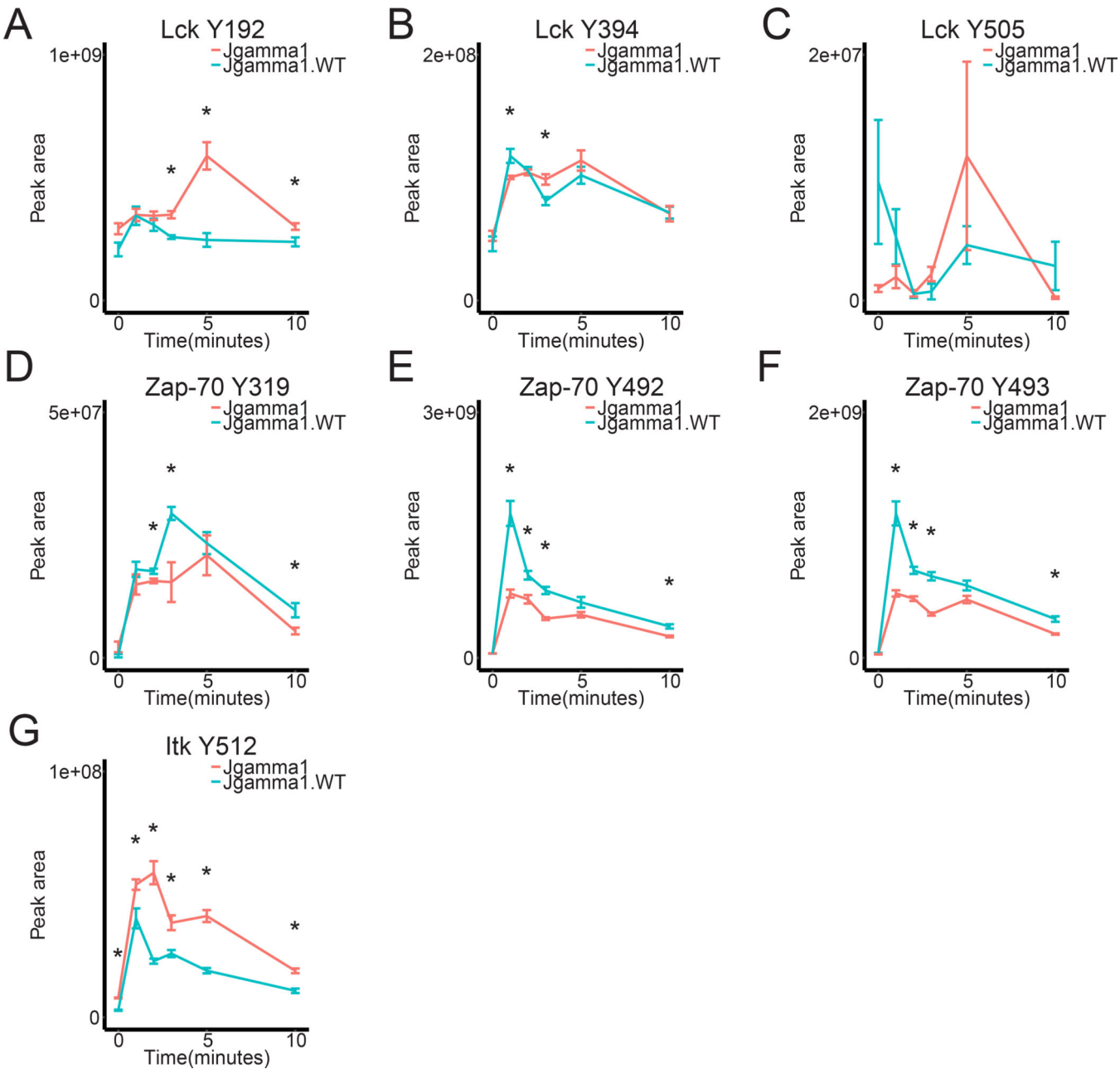

Figure 5.

Phosphorylation kinetics of regulatory tyrosine residues on Lck, Zap-7, and Itk. Phosphorylation kinetics of Lck regulatory sites A) Tyr^{192}, B) Tyr^{394}, and C) Tyr^{505}, Zap-7 D) Tyr^{319}, E) Tyr^{492}, F) Tyr^{493}, and Itk G) Tyr^{512} are depicted during early TCR signaling. Each data point represents the mean phosphopeptide abundance measured across five biological replicate experiments, and error bars indicate the standard error of the mean. Asterisks represent a statistically significant difference ($q < 0.05$) between Jgamma1 cells and Jgamma1.WT cells at the indicated time point.

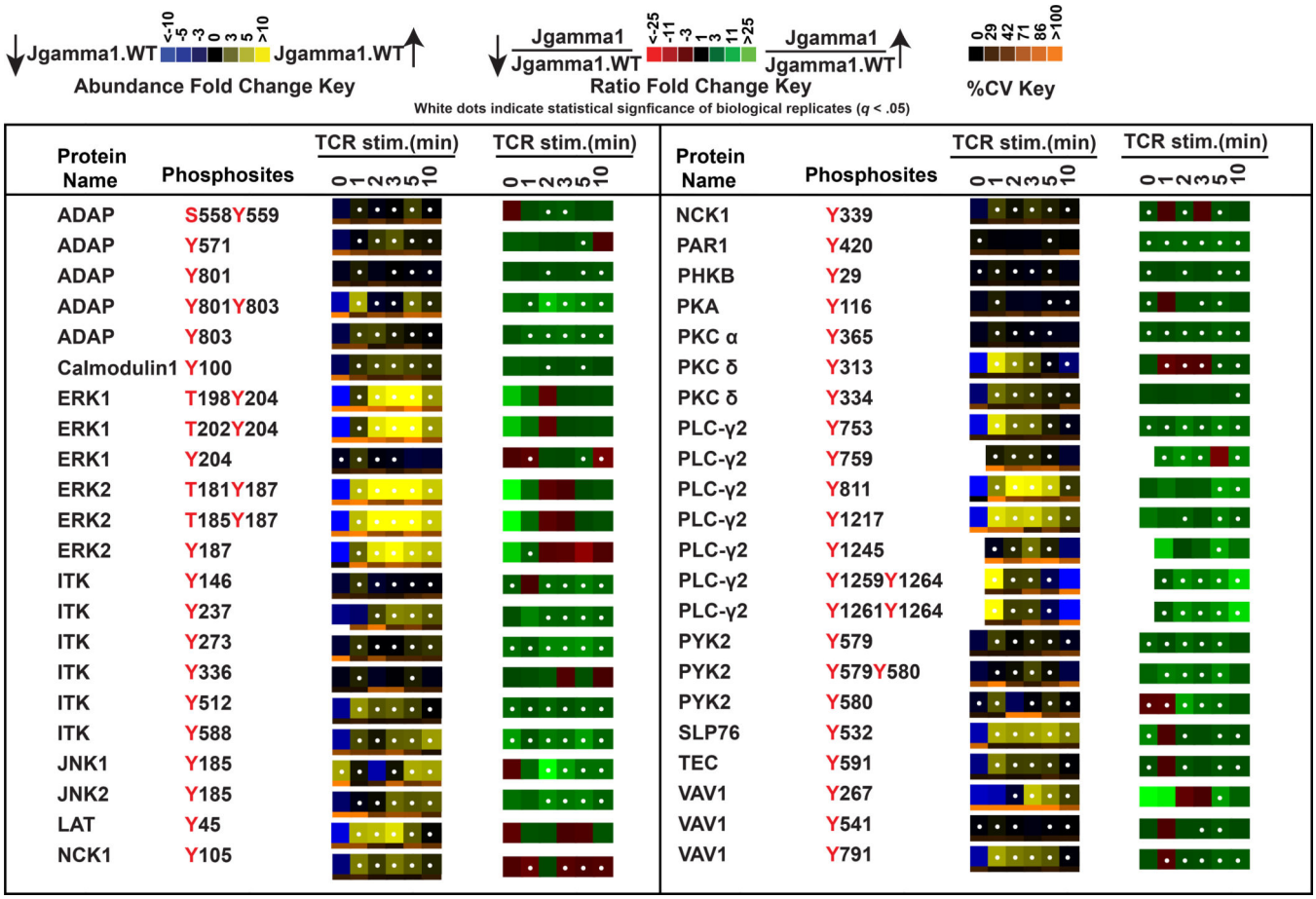

Figure 6.

Quantitative phosphoproteomic analysis of proteins within the calcium signaling pathway and SLP-76 multimolecular complex. Heatmaps were calculated from 5 biological replicate experiments. The interpretation of the heatmap color scheme as well as the white dots is described in Materials and Methods and identical to Figure 1.

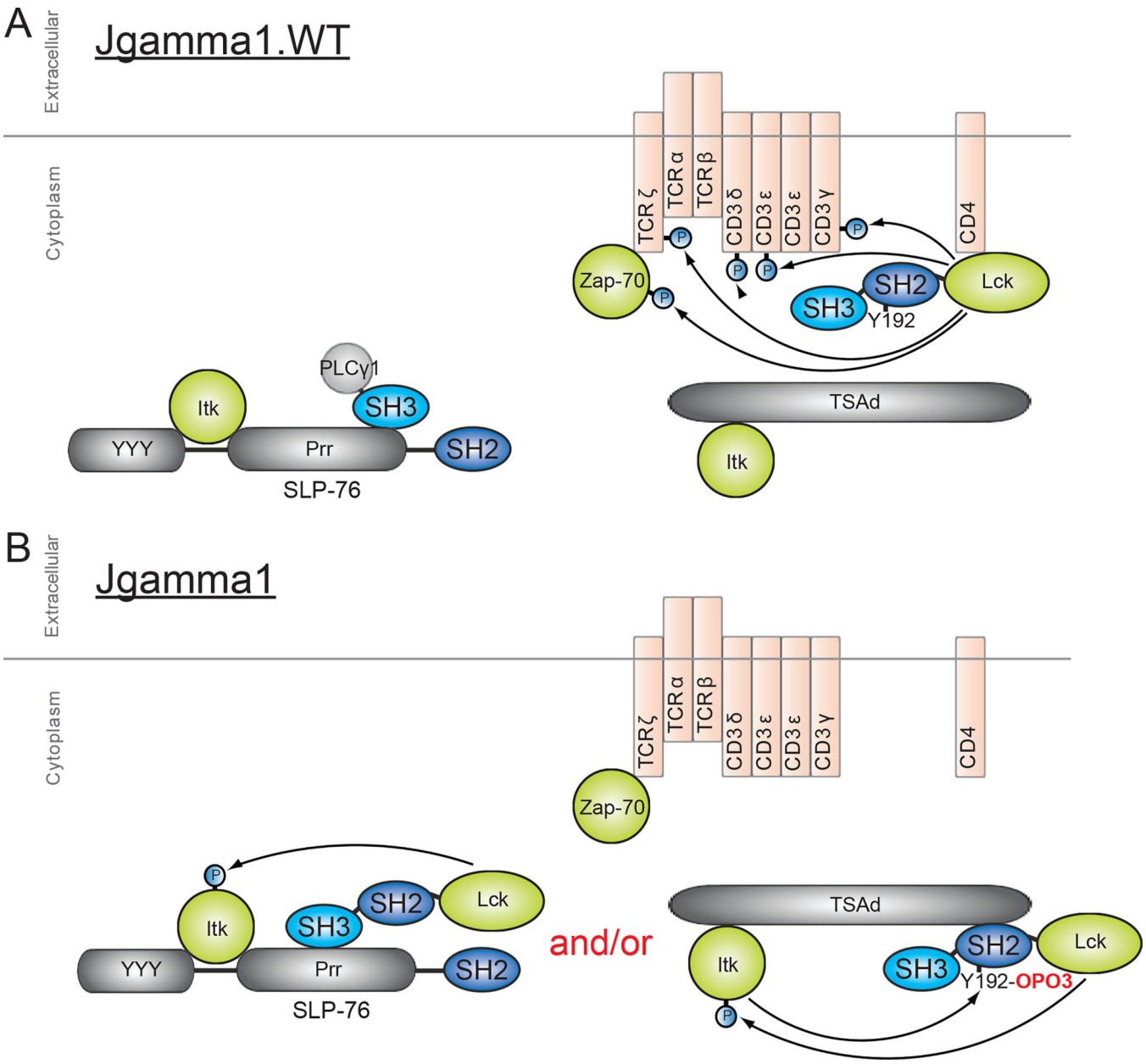

Figure 7.

Proposed model of early Lck-mediated phosphorylation events following TCR engagement in wild-type and PLC-γ1-deficient cells. PLC-γ1 is expanded to depict a single SH3 domain only. A) In reconstituted cells, Lck associates with the cytoplasmic tail of CD4. Upon engagement of the TCR, Lck phosphorylates the cytoplasmic tails of the receptor subunits, as well as activating residues on Zap-7. B) In the absence of PLC-γ1, Lck association with the proline-rich region of SLP-76 as well as TSAd is increased, bringing it into proximity with Itk. Reciprocal phosphorylation of Itk and Lck at Tyr^{512} and Tyr^{192} respectively reinforces the association of both kinases with the adaptors.